

*Alsumiri & Althomali, 2017*

*Volume 3 Issue 3, pp. 153-162*

*Date of Publication: 13<sup>th</sup> December 2017*

*DOI-<https://dx.doi.org/10.20319/mijst.2017.32.153162>*

*This paper can be cited as: Alsumiri, M & Althomali, R. (2017). Implementation of Sepic in Small Scale Wind Power Generation System. MATTER: International Journal of Science and Technology, 3(3), 153-162.*

*This work is licensed under the Creative Commons Attribution-Non Commercial 4.0 International License. To view a copy of this license, visit <http://creativecommons.org/licenses/by-nc/4.0/> or send a letter to Creative Commons, PO Box 1866, Mountain View, CA 94042, USA.*

## **IMPLEMENTATION OF SEPIC IN SMALL SCALE WIND POWER GENERATION SYSTEM**

**Mohammed Alsumiri**

*Department of Electrical and Electronics Engineering Technology, Yanbu Industrial College,  
Yanbu, Saudi Arabia  
[alsumiri@rcyci.edu.sa](mailto:alsumiri@rcyci.edu.sa)*

**Raed Althomali**

*Department of Electrical and Electronics Engineering Technology, Yanbu Industrial College,  
Yanbu, Saudi Arabia  
[althomalir@rcyci.edu.sa](mailto:althomalir@rcyci.edu.sa)*

---

### **Abstract**

*Wind power generation system in a small scale application considered as one of the cost effective solutions since the energy price increases. Also, it can be an alternative solution for people who live in rural areas, where they do not have access to the national grid. This research investigate the implementation of a Single-Ended Primary-Inductor Converter (SEPIC) in a Permanent Magnet Synchronous Generator (PMSG) based Wind Power Generation System (WPGS). Variable structure control has been employed to compensate the uncertainties in WPGS and to improve the energy conversion efficiency. This paper illustrates the dynamic model of the PMSG and the controller design. A simplified controller design based on an improved sliding surface has been presented. Maximum Power Point Tracking (MPPT) algorithm has been followed to harvest maximum energy from the wind. The results show satisfactory dynamic performance of the WPGS and maximum power coefficient has been achieved.*

## Keywords

MPPT, Sliding Mode, SEPIC, Wind Power Generation System

---

## 1. Introduction

Wind energy conversion system is a talented renewable resource of energy and it received many attentions especially when power electronics industry grows up. On the other hand, the high initial cost, the lower energy conversion efficiency and the non-linearity of the system variables limit WPGS applications. In order to overcome these limitations and to have an efficient energy conversion system MPPT is highly recommended. DC-DC converters are other key elements in the WPGS. There are a number of topologies, i.e. a boost converter that boosts the output voltage, a buck converter in which the voltage is stepped down and a buck-boost converter in which its output voltage varies from lower than or to higher than the voltage source. Apart from changing the voltage level, DC-DC converters received the control signal that ensures MPP achievement by varying the generator speed.

SEPIC is another topology of DC-DC converter and it is similar to the buck-boost converter in varying the output voltage. Furthermore, a capacitive isolation due to its construction protects the converter from switch failure; also due to its construction the output voltage always has the same polarity as the input voltage (El Shahat, 2012). Since the capacitors are used as main energy storage, the SEPIC draw an input current with least ripple (Alsumiri, 2016).

The small-scale WPGS employed in this research is based on direct driven PMSG. PMSG has many advantages for small-scale low cost applications such as, high voltage to inertia ratio, high air-gap flux density, and a high torque to volume ratio and the unneeded external DC supply to excite the generator windings that are not available in other generator types (Mahdi, 2010).

Based on high frequency switching and feedback, sliding mode control is competitive. SMC has various advantages over other conventional control such as: 1) inconsiderateness to system parameters variation, load changes and disturbance (Datta & Ranganathan, 2003); 2) robustness and immediate response (Vrdoljak, 2010). The structure of SMC involved a design of a sliding surface which needs to be stable and development of an optimal control law (Alsumiri, 2013). Achieving optimal control law design allows a finite time achievement of the operating

point to reach a predetermined sliding surface (Bandyopadhyay, 2009). The convergence of the control variable is guaranteed by introducing a constant gain which also, compensates the uncertainties of the control system (Alsumiri, 2016), (Gonzalez, 2012), (Levant, 2007).

This research investigates the dynamics of a PMSG based WPGS when SEPIC topology is implemented. Also in this research, a modified sliding surface has been designed. The organisation of the paper is as the following. In section 2, the WPGS modelling is demonstrated including Wind power model, PMSG model and analysis of the SEPIC. The proposed SMC controllers are discussed in section 3. The simulation results and analysis and are presented in Section 4, where research is concluded in Section 5.

## 2. WPGS Model

WPGS, which is investigated, is illustrated in Fig. 1. It consists of a vertical axis wind turbine directly coupled to a PMSG. The 3-phase voltage from the PMSG is rectified through an uncontrolled 3- phase six pulse diode rectifier. The DC output voltage is boosted and regulated using SEPIC. The measured end wind speed, rotor speed and 3-phase AC voltage and currents are used by the control system. The control signal is generated to control the duty cycle of the SEPIC. The SEPIC output voltage is fed to a stand-alone load.

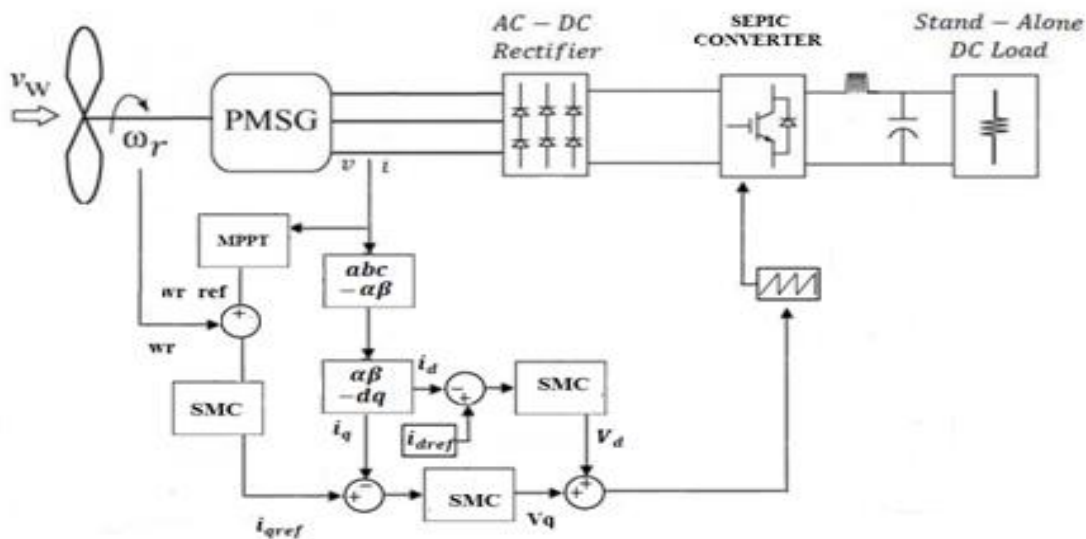


Figure 1: The Employed WGS Block Diagram

## 2.1 Wind Turbine Model

Wind ( $P_w$ ), stores kinetic energy which is directly proportional to the wind turbine swept area ( $A$ ), air density ( $\rho$ ) and wind speed ( $V_w$ ) cube (Burton, 2011). Mechanical power ( $P_m$ ) from the wind turbine could be calculated by introducing the power coefficient ( $C_p$ ) and multiplied by the wind power.

$$P_w = \frac{1}{2} \rho A V_w^3, (1)$$

$$P_m = \frac{1}{2} \rho A C_p V_w^3. (2)$$

The power coefficient calculations depend on the wind turbine type, i.e. horizontal axis or vertical axis.  $C_p$  is a function of the tip speed ratio (TSR), which is the ratio of the speed of the wind in meter per second to the rotational speed. The calculated wing power coefficient based on TSR for the vertical axial wind turbine can be shown in the following equations.

$$C_p = -0.13\lambda^3 - 0.12\lambda^2 + 0.45\lambda, \quad \lambda = \frac{\omega_r R}{V_w}, (3)$$

where,  $\omega_r$  is the mechanical rotation speed,  $\lambda$  is the TSR and  $R$  is the rotor radius of the wind turbine.

## 2.2 PMSG Model

The d-q synchronous reference frame for the employed PMSG is developed by aligning the d-axis to magnetic axis, where the q-axis is orthogonal to the d-axis (Jiang, 2005). The dynamic PMSG model in synchronous d-q reference frame can be demonstrated as follows:

$$V_d = R_s i_d + L_d \frac{di_d}{dt} - \omega_e L_q i_q, (4)$$

$$V_q = R_s i_q + L_q \frac{di_q}{dt} + \omega_e (L_d i_d + \psi_{PM}), (5)$$

Where,  $d$  denote quantities in the d-axis and  $q$  represent them in the q-axis, for voltage ( $V$ ), current ( $i$ ) and inductance ( $L$ ). The electrical speed in radians per second is ( $\omega_e$ ) while, the flux for the permanent magnet is indicated by ( $\psi_{PM}$ ). The descriptions of the PMSG behavior are listed below:

$$T_m = T_e + J \frac{d\omega_r}{dt} + B \omega_r, \quad \omega_e = p \omega_r, (6)$$

$$T_e = 1.5p[\psi_{PM} i_q + (L_d - L_q) i_d i_q], (7)$$

Where ( $m$ ) and ( $e$ ) denote the mechanical and electrical quantities for torque ( $T$ ). The inertia of the PMSG and the viscous friction coefficient are ( $B, J$ ) respectively. The pole pairs are indicated by ( $p$ ).

### 2.3 SEPIC Model

SEPIC can achieve the performance of DC-DC buck converter and also it can act as DC-DC boost converter, in which the polarity of the output voltage is kept the same as the input voltage, by varying the duty cycle. Having low input current ripple is a nature of SEPIC and this will lead to significant improvement in the average value of power. The SEPIC is designed to have an IGBT switch ( $S_1$ ). In the output a diode (D) is placed. The construction of SEPIC also includes capacitors ( $C_1$  and  $C_o$ ) and inductors ( $L_1$  and  $L_2$ ). The exchanged energy between the capacitors and inductors permit SEPIC to have a wide variation in the output voltage. It worth to note that the voltage rating of a series coupling capacitor ( $C_1$ ) should exceed the input voltage level in order to permit energy transformation from input to output (Mohammad, 2013). Typical SEPIC is shown in Fig. 2 (a) including both states of actions i.e. OFF (b) and ON (c). Hence, SEPIC operations can be described as below:

- ON STATE

$$L_1 \frac{di_1}{dt} = V_{in}, C_2 \frac{dv_o}{dt} + \frac{v_o}{R} = 0, (8)$$

- OFF STATE

$$L_1 \frac{di_1}{dt} + V_{c1} + V_o = V_{in}, i_1 - i_2 - C_2 \frac{dv_o}{dt} - \frac{v_o}{R} = 0. (9)$$

By averaging ON and OFF states and introducing the duty cycle (D), the demonstration can be as the following:

$$L_1 \frac{di_1}{dt} = V_{in} - \left[ (V_{c1} + V_o) \left( \frac{1-D}{D} \right) \right], C_2 \frac{dv_o}{dt} = (i_1 - i_2) \left( \frac{D}{1-D} \right) - \frac{V_o}{R}. (10)$$

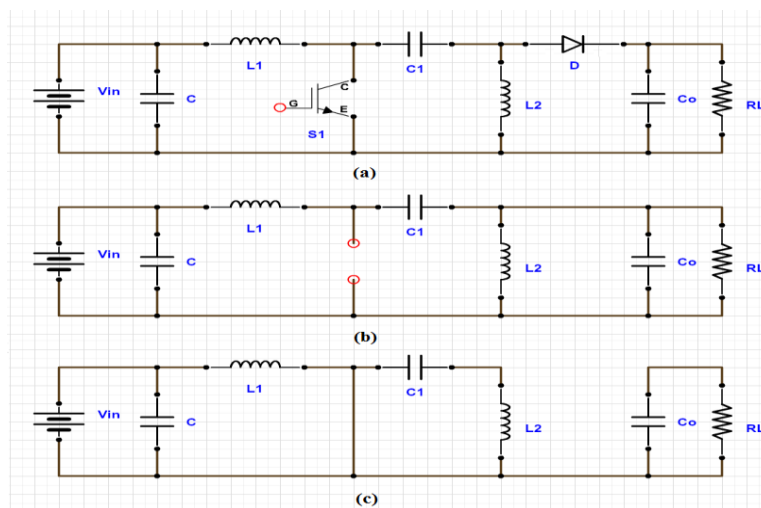


**Figure 2:** (a) SEPIC, (b) OFF state and (c) ON state

### 3. Controller Design

In this research, the d-q axis currents are controlled to their reference using SMC controllers. The field oriented control has been implemented by aligning the quadrature current component to the flux of the rotor and setting the direct current component to zero (Alsumiri, 2013). The decoupled PMSG model can be as below:

$$V_d = R_s i_d + L_d \frac{di_d}{dt}, \quad (11)$$

$$V_q = R_s i_q + L_q \frac{di_q}{dt}. \quad (12)$$

The mechanical speed is also controlled using SMC loop. The mechanical speed control loop generates a reference signal to the q-axis current control. The sliding surface is developed to be the PI error structure between the reference speed which is generated from the MPPT and the actual speed of the generator. The structure of the SMC can be shown as the following (Castaños & Fridman 2006):

$$s(x) = k_p e + k_i \int e \, dt, \quad e = x_{ref} - x, \quad (13)$$

where,  $(s)$  denotes sliding surface.  $(k_p)$  and  $(k_i)$  are constants. The difference between reference value  $(x_{ref})$  and a controlled variable  $(x)$  is the error  $(e)$ . Equivalent control which is a commonly acknowledged approach in analysing the motion during SM (Bandyopadhyay, 2009) is followed in controller design. The aim is to substitute the discontinuity nature, which makes  $\dot{s}(0)$  move toward 0, by an equivalent control that is by making  $\dot{s}(x) = 0$ . So that, the structure of the SMC can be demonstrated as (Alsumiri, 2013):

$$u = u_{eq} + u_n, \quad (14)$$

where,  $u_{eq}$  is the equivalent control element and it can be calculated along the sliding mode as follows,

$$\dot{s}(x) = 0, \quad (15)$$

$$u_n = -K \operatorname{sign}(s), \quad (16)$$

$$\operatorname{sgn}(x) = \begin{cases} 1, & s > 0 \\ 0, & s = 0 \\ -1, & s < 0 \end{cases}. \quad (17) \text{ Where, } (K) \text{ is SM constant.}$$

#### 3.1 Speed Control Design

The speed design equations can be expressed as follows:

$$e_w = \omega_{ref} - \omega_r, \quad (18)$$

$$s(\omega_r) = k_p e_w + k_i \int e_w de, \quad (19)$$

$$\dot{s}(\omega_r) = k_p \dot{e}_w + k_i e_w, \quad (20)$$

$$\dot{s}(\omega_r) = k_p \dot{\omega}_{ref} + k_i \omega_{ref} - k_i \omega_r - \frac{k_p T_m}{J} + \frac{k_p 1.5 \rho \psi_{PM}}{J} i_q + \frac{k_p B}{J} \omega_r. \quad (21)$$

The equivalent speed control equation which governs the speed control loop can be shown as below:

$$u = i_q^* = \frac{1}{1.5 \rho \psi_{PM}} (J T_m - J \dot{\omega}_{ref} - B \omega_r) + \frac{J}{1.5 \rho \psi_{PM}} \frac{k_i}{k_p} (e_w) - K \text{sign}(e_w), \quad (22)$$

By introducing  $k_s$ , which can replace the gains above since the SMC can compensate the uncertainties. The equivalent control equation can be rearranged as follows:

$$u = i_q^* = \frac{1}{1.5 \rho \psi_{PM}} (J T_m - J \dot{\omega}_{ref} - B \omega_r) + k_s [(e_w) - \text{sign}(e_w)]. \quad (23)$$

### 3.2 d-q current Control Design

Similarly the d-q axis currents are controlled to their reference values using SMC using the modified sliding surface. The equivalent control equations for the d-q currents control are as below:

$$u = V_d^* = L_d \dot{I}_{dref} + R_a I_d - L_d \omega_e I_q + k_d [(e_d) - \text{sign}(e_d)], \quad (24)$$

$$u = V_q^* = L_q \dot{I}_{qref} + R_a I_q + \omega_e (L_q I_d + \psi_{PM}) + k_q [(e_q) - \text{sign}(e_q)]. \quad (25)$$

## 4. Simulation Results and Analysis

The proposed control system of the WPGS is shown in Fig. 1. The simulation of the system dynamics has been done using MATLAB/SIMULINK. Analysis of transient response and controller robustness has been conducted. Figure 3 illustrates the mechanical rotational speed of the WPGS. It can be noted from the figure that PMSG speed perfectly tracks its reference signal which is generated from the MPPT controller. Still, chattering effect appears in the speed as well as small overshoot error during transient for high wind speeds. However, the controller forces the speed to track its reference and MPPT operations are achieved. The TSR and the power coefficient are illustrated in Fig. 4. The TSR and the power coefficient are at their optimum values of 0.822 and 0.22 respectively, which indicates successful achievement of MPPT operation.

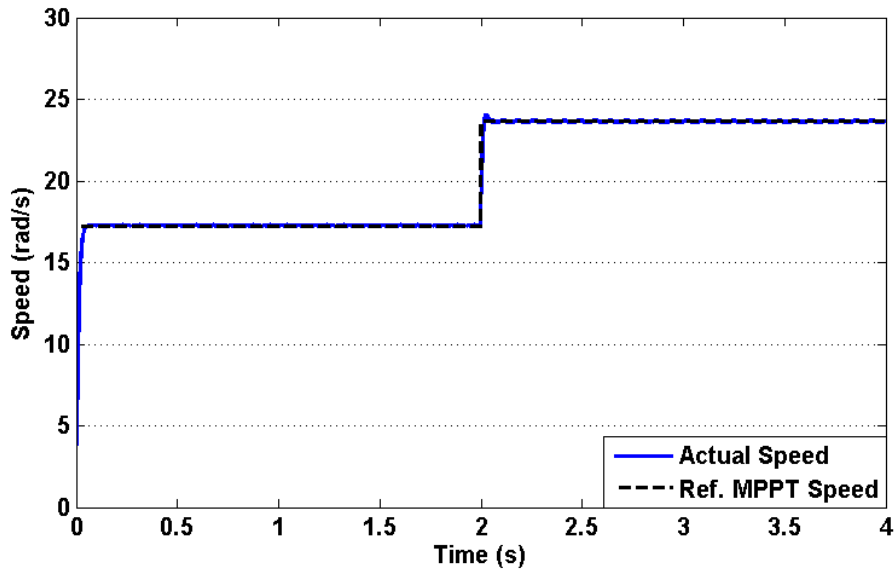


Figure 3: Actual Speed Tracking Reference Speed

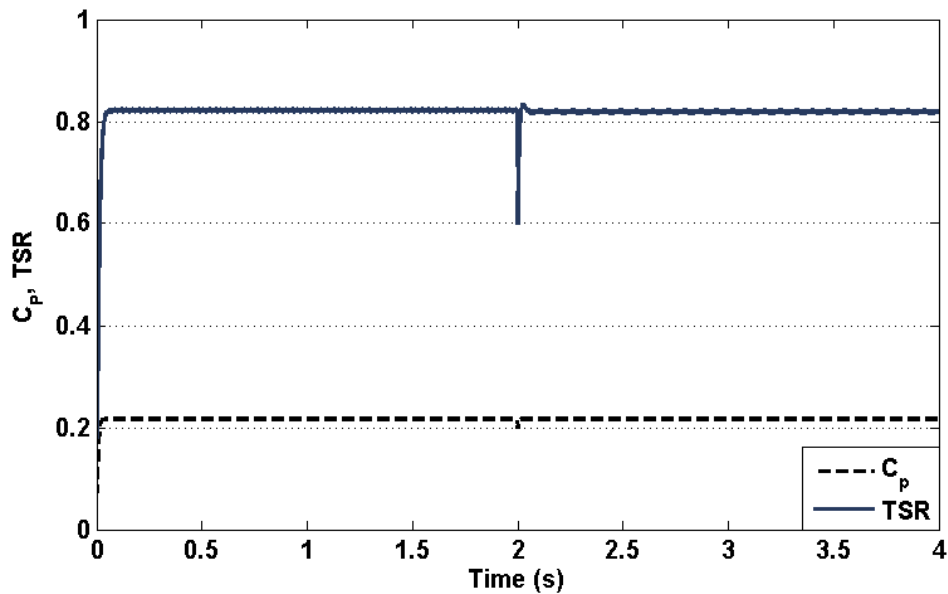


Figure 4: Power Coefficient and TSR

## 5. Conclusion

This research focus on the investigation of SEPIC in PMSG based WPGS. The PMSG has been controlled using SMC. The design of the speed control loop and d-q currents control loops are illustrated. The WPGS system has been simulated and analyzed. The results shows satisfactory dynamics with reduced chattering and minimum overshoots.

## References

- Alsumiri, M. A., Tang, W. H., & Wu, Q. H. (2013, December). Maximum Power Point Tracking for Wind Generator System Using Sliding Mode Control. In Power and Energy Engineering Conference (APPEEC), 2013 IEEE PES Asia-Pacific (pp. 1-6). IEEE.  
<https://doi.org/10.1109/APPEEC.2013.6837183>
- Alsumiri, M. A., & Jiang, L. (2016). Sliding Mode Maximum Power Point Tracking Controller for Photovoltaic Energy Conversion System with a SEPIC Converter. In Proceedings of the Eighth Saudi Students Conference in the UK (pp. 463-475).  
[https://doi.org/10.1142/9781783269150\\_0040](https://doi.org/10.1142/9781783269150_0040)
- Bandyopadhyay, B., Deepak, F., & Kim, K. S. (2009). Sliding mode control using novel sliding surfaces (Vol. 392). Springer. <https://doi.org/10.1007/978-3-642-03448-0>
- Burton, T., Jenkins, N., Sharpe, D. & Bossanyi, E. (2011), Wind energy handbook, John Wiley & Sons. <https://doi.org/10.1002/9781119992714>
- Castanos, F. & Fridman, L. (2006), 'Analysis and design of integral sliding manifolds for systems with unmatched perturbations', Automatic Control, IEEE Transactions on 51(5), 853–858. <https://doi.org/10.1109/TAC.2006.875008>
- Faranda, R. & Leva, S. (2008), 'Energy comparison of mppt techniques for pv systems', WSEAS transactions on power systems 3(6), 446–455.
- Datta, R. & Ranganathan, V. (2003), 'A method of tracking the peak power points for a variable speed wind energy conversion system', Energy conversion, IEEE transactions on 18(1), 163–168. <https://doi.org/10.1109/TEC.2002.808346>
- El Shahat, A. (2012), 'Stand-alone pv system simulation for dg applications', Journal of Automation & Systems Engineering 6(1), 55–72.
- Gonzalez, T., Moreno, J. A. & Fridman, L. (2012), 'Variable gain super-twisting sliding mode control', Automatic Control, IEEE Transactions on 57(8), 2100–2105.  
<https://doi.org/10.1109/TAC.2011.2179878>
- Jiang, S., Liang, J., Liu, Y.-d., Yamazaki, K. & Fujishima, M. (2005), Modeling and cosimulation of fpgabasedsvpwm control for pmsm, in 'Industrial Electronics Society, 2005. IECON 2005.31st Annual Conference of IEEE', IEEE, pp. 6–pp.
- Levant, A. (2007), 'Principles of 2-sliding mode design', Automatica 43(4), 576–586.  
<https://doi.org/10.1016/j.automatica.2006.10.008>

- Mahdi, A., Tang, W. & Wu, Q. (2010), Improvement of a mppt algorithm for pv systems and its experimental validation, in ‘International Conference on Renewable Energies and Power Quality, Granada, Spain’. <https://doi.org/10.24084/repqj08.419>
- Mohammad, N., Quamruzzaman, M., RubaiyatTanvir Hossain, M. &RafiqulAlam, M. (2013), ‘Parasitic effects on the performance of dc-dc sepic in photovoltaic maximum power point tracking applications.’, Smart Grid & Renewable Energy 4(1).
- Vrdoljak, K., Peri´c, N. & Petrovi´c, I. (2010), ‘Sliding mode based load-frequency control in power systems’, Electric Power Systems Research 80(5), 514–527.  
<https://doi.org/10.1016/j.epsr.2009.10.026>